Experimental Investigations of the Controlled Motion of the Roller Racer Robot

Alexander Kilin[1], Yuriy Karavaev[2], and Kirill Yefremov[2(✉)]

[1] Ural Mathematical Center, Udmurt State University, Izhevsk, Russia
aka@rcd.ru
[2] Kalashnikov Izhevsk State Technical University, Izhevsk, Russia
karavaev_yury@istu.ru

Abstract. In this paper we presents the results of experimental investigations and simulations of the motion of the Roller Racer. We assume that the angle $\varphi(t)$ between the platforms is a prescribed function of time and that the no-slip condition (nonholonomic constraint) and viscous friction force act at the points of contact of the wheels. The results of theoretical and experimental investigations are compared for various values of the parameters of the control action and design parameters of mobile robot.

Keywords: Roller Racer · Nonholonomic constraint · Viscous friction · Control · Periodic solution

1 Introduction

The Roller Racer is a mobile robot consisting of two platforms that can rotate in a horizontal plane relative to each other. Each platform has a rigidly attached wheel pair consisting of two passive wheels lying on the same axis. The propulsion of the Roller Racer is possible due to periodic rotation of the platform relative to each other. A similar principle of movement is used by snake-like robots. But they consist of many actuated joints. For comparison, the roller racer has only one motor, opposite two for the most spread mobile robot with a differential drive or snake-like robot. This reduces the cost of the design of such a robot, but complicates the control system.

In the general form, the dynamics of the inertial motion of the Roller Racer is examined in [4]. The equations of motion of the Roller Racer involve a large number of parameters. Therefore, as a rule, this system is considered under some restrictions on the position of the center of mass of each platform [1–3]. In this work, we assume that the center of mass of each platform is on its symmetry axis and two principal axes of inertia lie in the plane parallel to the plane of rolling of the system.

The authors of [5] consider the problem of the motion of the system for the angle $\varphi(t)$ between the platforms as a prescribed periodic function of time.

D. Chugo et al. (Eds.): CLAWAR 2021, LNNS 324, pp. 428–437, 2022.
https://doi.org/10.1007/978-3-030-86294-7_38

Equations of motion are obtained for fairly general mass distribution of the platforms. It is proved that, in the general case, when the viscous friction forces act on the system at the point of contact of the wheels with the plane, there is no constant acceleration of the Roller Racer and all trajectories of the reduced system asymptotically tend to a periodic solution.

In paper [9] a complete classification of possible types of motion of a wheeled vehicle with two wheel pair is presented and their dynamics are analyzed for two particular cases: a symmetric vehicle with one fixed axle and a symmetric vehicle with unfixed axles. Similar systems are investigated also in [10–12].

In this paper, the results of experimental and theoretical investigations of the motion of the mobile robot with the design of the Roller Racer were presented. We investigate the influence of design parameters and the parameters of the control action on the velocity of the robot's motion. Taking into account the technical restrictions of rotation angle φ, torque and angular velocity of the driving motor we determinate the values of parameters of control action and relation of axial moments of inertia of platforms to provide the maximum velocity of propulsion.

2 Equations of Motion

Consider the problem of the motion of the Roller Racer on a plane relative to an inertial coordinate system Oxy. The plane Oxy coincides with the plane of motion (Fig. 1).

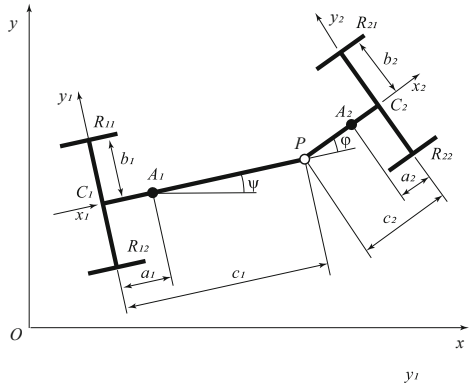

Fig. 1. The Roller Racer on a plane

Where φ is the angle between the axes C_1x_1 and C_2x_2 (the orientation of the platforms relative to each other, ψ is the angle between the axes Ox and C_1x_1 (the orientation of the first platform relative to the fixed coordinate system), h is the radius of the wheels on the first and second platforms in the fixed coordinate system Oxy, c_1, c_2 are distances from the center of the first and second wheel

pairs to point P, a_1, a_2 are distances from point C_1 to the center of mass of the first platform and from point C_2 to the center of mass of the second platform, m_1, m_2 are the masses of the first and second platforms, I_{10}, I_{20} are the moments of inertia of the first and second platforms relative to their centers of mass (points A_1 and A_2), b_1, b_2 are distances from the point of contact of the wheels to the center of mass of the corresponding wheel pair.

We assume that there is no slipping at the points of contact of the wheels with the x-y plane. The corresponding constraint equations can be written in the form [5]

$$\begin{gathered} -\dot{x}\sin\psi + \dot{y}\cos\psi + c_1\dot{\psi} = 0, \\ -\dot{x}\sin(\varphi(t)+\psi) + \dot{y}\cos(\varphi(t)+\psi) - c_2(\dot{\varphi}(t)+\dot{\psi}) = 0. \end{gathered} \tag{1}$$

These relations mean that the projection of the velocity of the center of mass of each wheel pair C_1 and C_2 onto the direction perpendicular to the plane of the corresponding wheel is equal to zero (see also [13]).

Instead of the generalized velocities $\dot{\boldsymbol{q}} = (\dot{x}, \dot{y}, \dot{\psi})$, it is convenient in this case to pass to the quasi-coordinates $\boldsymbol{v} = (v_1, v_2)$ and ω, where $\boldsymbol{v}$ is the velocity of point P referred to the axes of the moving coordinate system $C_1x_1y_1$, and ω is the absolute angular velocity of the first platform:

$$v_1 = \dot{x}\cos\psi + \dot{y}\sin\psi, \quad v_2 = -\dot{x}\sin\psi + \dot{y}\cos\psi, \quad \omega = \dot{\psi}.$$

The constraint Eq. (1) in the new variables become

$$\begin{gathered} v_2 + c_1\omega = 0, \\ v_1\sin\varphi(t) - v_2\cos\varphi(t) + c_2(\omega + \dot{\varphi}(t)) = 0. \end{gathered} \tag{2}$$

In [5] it is shown that in the case where the angle $\varphi(t)$ between the platforms is a prescribed function of time, the equation governing the evolution of the linear velocity of the first platform v_1 can be written as

$$\dot{v}_1 = \big(A(t) - C(t)\big)v_1 + B_1(t) + B_2(t) - D(t), \tag{3}$$

where

$$\begin{gathered} A(t) = -\frac{\dot{\varphi}\sin\varphi(J_1S_2 + \delta S_1)}{S_1(J_1\sin^2\varphi + MS_1^2)}, \\ B_1(t) = \frac{\ddot{\varphi}\sin\varphi(J_1c_2 - J_2S_1)}{(J_1\sin^2\varphi + MS_1^2)} \\ B_2(t) = \frac{\dot{\varphi}^2(J_1c_1c_2\sin^2\varphi - S_1(c_1\delta\cos\varphi + \varepsilon c_2S_1))}{S_1(J_1\sin^2\varphi + MS_1^2)} \\ C(t) = 2\frac{(b_1^2k_1 + b_2^2k_2)\sin^2\varphi + k_1S_1^2 + k_2S_2^2}{J_1\sin^2\varphi + MS_1^2}, \\ D(t) = 2\frac{\dot{\varphi}\sin\varphi\big(c_1k_2(b_2^2 - c_2^2)\cos\varphi - c_2(b_1^2k_1 + c_1^2k_2)\big)}{J_1\sin^2\varphi + MS_1^2}, \\ S_1 = c_1\cos\varphi + c_2, \quad S_2 = c_1 + c_2\cos\varphi. \end{gathered}$$

Here, to abbreviate the formula, we have introduced the following notation:

$$M = m_1 + m_2, \quad \delta = c_1 a_2 m_2 + c_2 a_1 m_1,$$
$$\varepsilon = m_1 a_1 + c_1 m_2, \quad k_1 = \frac{\kappa_1}{h^2}, \quad k_2 = \frac{\kappa_2}{h^2},$$
$$J_1 = I_{10} + I_{20} + m_1 a_1^2 + m_2(a_2^2 + c_1^2 - c_2^2),$$
$$J_2 = I_{20} - m_2(c_2^2 - a_2^2).$$

Where $k_1 > 0$ and $k_2 > 0$ are positive (friction) coefficients. Investigations of similar mechanical systems in presents of viscous rolling resistance is considered in works [6,7]. The coefficient of friction was determined for the condition of minimizing the deviation of the simulated trajectory from the experimental one, by analogy with the work [8]. The evolution of the configuration variables is governed by the system

$$\dot{\psi} = -\frac{v_1 \sin\varphi(t) + c_2\dot{\varphi}(t)}{c_1 \cos\varphi(t) + c_2},$$
$$\dot{x} = v_1 \cos\psi - c_1 \frac{v_1 \sin\varphi(t) + c_2\dot{\varphi}(t)}{c_1 \cos\varphi(t) + c_2} \sin\psi, \tag{4}$$
$$\dot{y} = v_1 \sin\psi + c_1 \frac{v_1 \sin\varphi(t) + c_2\dot{\varphi}(t)}{c_1 \cos\varphi(t) + c_2} \cos\psi.$$

The angle $\phi(t)$ between the platforms is used as a control action. In next section, the influence of the mass-inertia parameters of the platforms and the control parameters on the velocity of propulsion of the Roller Racer are considered.

3 Experimental Part

Experimental validation of the proposed model with viscous rolling resistance in case of periodical control action was obtained in [15]. Continuing those studies we consider the prototype of the Roller Racer which allows us to change the mass distribution at each platform or change their axial moments of inertia. The 3D model and fabricated prototype are shown in Fig. 2. The values of the mass-inertia parameters of fabricated prototype used also in simulations are presented in Table 1. As design parameters in this paper we consider the ratio of the axial moments of inertia of the platform J_{20}/J_{10}. The mass of the first platform is constant. The mass of second platform is variable by adding loads to the special places located on the second platform. As a control action we use the periodic function:

$$\varphi(t) = \alpha \cdot sin(\frac{2\pi t}{T}) + \varphi_0, \tag{5}$$

where T is the period of function, α is an amplitude, φ_0 the vertical of the function shift. For control of the Roller Racer, a control board based on the STM32F303K3C6 microcontroller is developed. To control the angle between of half-frames, a CDS5516 servo drive is used. The servo drive powered by a

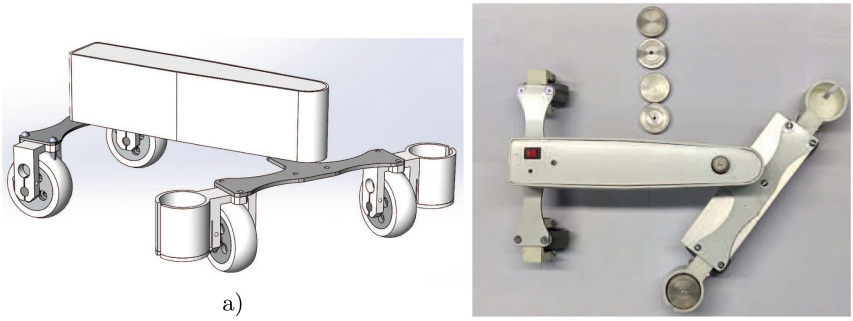

a) b)

Fig. 2. Prototype the Roller Racer a) 3d model of robot b) picture of prototype with loads

Table 1. The values of parameters of Roller Racer

Parameter	Value
Maximum amplitude of rotation angle between the platforms φ, rad	2.6
Maximum angular velocity $\dot{\varphi}$, rpm	30
The mass of the first platform (without additional load), kg	0.469
The mass of the second platform, kg	0.250
The mass of one load, kg	0.066
The axial moment of inertia of the first platform I_{10} (relative to the vertical axis passing through the center of mass of the first platform), kg $\cdot$ m^2	0.00386
The axial moment of inertia of the second platform I_{20} (relative to the vertical axis passing through the center of mass of the second platform, kg $\cdot$ m^2	0.00175
The distance from the center of mass of the first platform to the point P $(c_1 - a_1)$, m	0.186
The distance from the center of mass of the second platform to the point P $(c_2 - a_2)$, m	0.0441
Coefficient of viscous friction κ	0.25

LiPo 2S battery. The servo is connected to the control board via a half-duplex UART. The speed of the serial port of the controller is 1 Mbps, the frequency of updating the status of the servo 250 Hz. The frequency of the update cycle of the robot control system 125 Hz for $T = 0.8$ s, 67 Hz for $T = 1.6$ s.

There are two types of motion depending on the value of φ_0. In case of $\varphi_0 = 0$ the robot moves along a straight line, and if $\varphi_0 \neq 0$ the trajectory of motion is a curve, which radius is defined by the value of φ_0.

3.1 Motion Along a Straight Line

Since the control function has a periodic character the point P oscillates along a trajectory during the robot's motion. For evaluation of the motion we calculate an average velocity of the Roller Racer over the period of oscillation. The data for calculation of the position and velocity is obtained by the Vicon motion capture system. The capture frequency of the motion capture system 100 Hz, the marker recognition error does not exceed 1 mm.

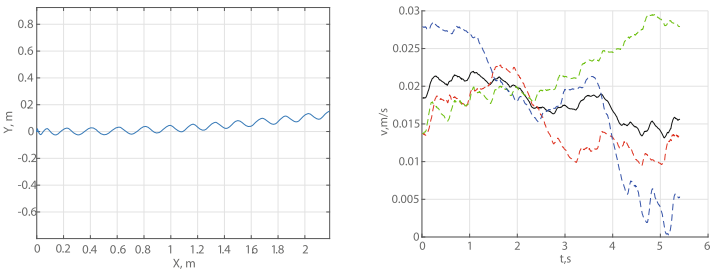

Fig. 3. A typical graph of the trajectory (a) and the average velocity of movement (b) of the robot. The dashed lines show the speeds obtained experimentally, without taking into account acceleration and deceleration. The solid line shows the average speed of the robot for three experiments with the same initial conditions.

The variability of the average velocity is explained by the influence of manufacturing errors of the robot, non-roughness of the underlying surfaces, etc. [14].

To investigate the theoretical model of the robot's motion two simulation series were carried out taking into account the mass-inertia parameters of the prototype: 1) the dependence of the average velocity on the ratio of the moments of inertia J_{20}/J_{10} for various values of α; 2) the dependence of the average velocity on the amplitude and the period of the control function (5). Each experiment is conducted at least three times. The average speed is calculated as the movement of the point P over the period of the control function T. The statistical analysis of the results consisted of calculating the confidence intervals for the mean-based results. The mean-based results is analysed using the standard equation for 95% confidence level and sample size - 3.

For the first experiments the period of the control function was taken T = 1 s, and the values of the amplitude of the rotation of the platform were taken from interval [0; 1.4] by step 0.05. The ratio of axial moments of inertia J_{20}/J_{10} was changed by attachment of the additional loads as follows: 0.08; 0.14; 0.17; 0.19; 0.2. Figure 4 shows the results of simulations and experimental investigations with real prototype. The experimental values are marked by the circle.

A minor deviation of the experimental values from the theoretical ones confirms the adequacy of the model and its ability to describe the motion by various

control and inertia parameters. The numerical results of experiments with confidence intervals are shown in the Table 2.

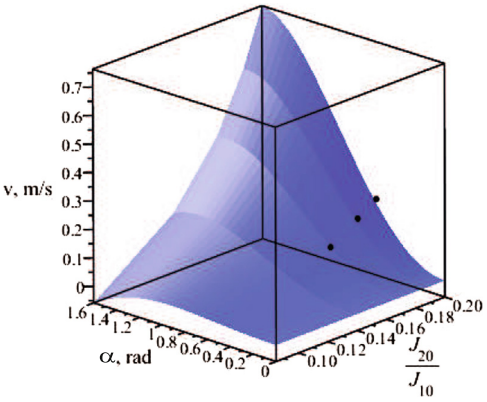

Fig. 4. Average velocity of Roller Racer versus ratio of the moments of inertia and the amplitude of the rotation angle between platforms

Table 2. The numerical results for first series of experiments

J_{20}/J_{10}	$\overline{v} \pm t_{\alpha,n-1} * \frac{\sigma}{\sqrt{n}}$, m/s	v_{exp}, m/s
0.16	0.1015 ± 0.056	0.1057
0.18	0.1659 ± 0.085	0.1511
0.2	0.2099 ± 0.096	0.1954

In another series of experiments we change the period of control from the interval T = [0.8; 2] s, by step 0.05 and the amplitude $\alpha = [0; 1.2]$ rad by 0.1 rad for the ratio of moments of inertia $J_{20}/J_{10} = 0.3$. The surface of results of the simulation with the experimental data are shown in Fig. 5. The numerical results of experiments with confidence intervals are shown in the Table 3.

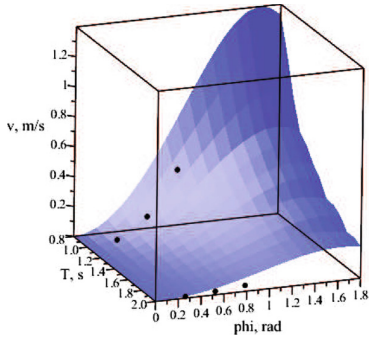

Fig. 5. Average velocity of Roller Racer versus period of the control function and the amplitude of the rotation angle between platforms.

Table 3. The numerical results for second series of experiments

T, s	α, rad	$\overline{v} \pm t_{\alpha,n-1} * \frac{\sigma}{\sqrt{n}}$, m/s	v_{exp}, m/s
1	0.262	0.0181 ± 0.015	0.027
1	0.524	0.1378 ± 0.046	0.16
1	0.785	0.3473 ± 0.124	0.45
2	0.262	0.0069 ± 0.006	0.011
2	0.524	0.0348 ± 0.024	0.023
2	0.785	0.0536 ± 0.014	0.04

According to the graphs shown in Figs. 5 and 4 we can conclude that the angular velocity of the robot increase when frequency of oscillation $1/T$ increases as well as the amplitude oscillations increases up to a certain value (about 1 rad, for our prototype). When the value of the amplitude increase more than this value the average velocity decreases first, and then the robot moves in opposite direction. According to the Tables 2 and 3 we can conclude that the simulation results are located within confidence intervals.

3.2 Movement of the Roller Racer Along a Circle

In the case of $\varphi_0 \neq 0$ the robot moves along a circle. Experiments and simulations were carried out with the same mass-inertia parameters of the prototype as for movement along the straight line and the ratio of moments of inertia was equal 0.3. The values of the $\varphi_0 \neq 0$ lie within the interval $[-\pi; \pi]$. The trajectories of motion obtained from the experiments and simulations for the values of parameters $\alpha = 0.52$, T = 1, $\varphi_0 = [0{,}0873;\ 0{,}174533;\ 0{,}261799]$ are presented in Fig. 6. The experimental data is shown by dashed lines.

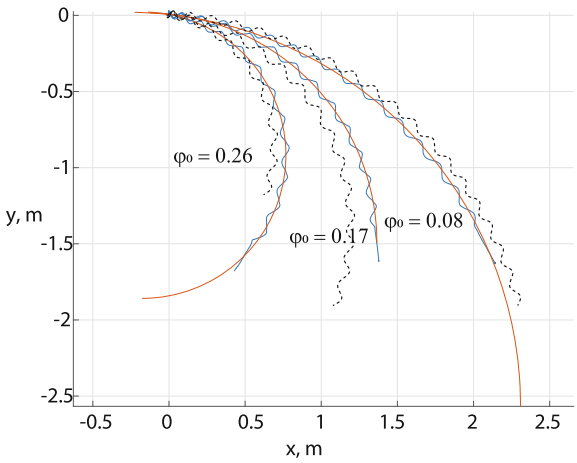

Fig. 6. Trajectories of movement with different shift of the control function. Dashed lines present theoretical trajectories. Solid lines present experimental trajectories.

The sign of the φ_0 defines the direction of motion. By increasing the value of $\varphi_0 \in [0; \pi]$ the radius of curvature of the trajectory of the robot decreases respectively.

4 Conclusions

The paper observed the results of simulations and experimental studies of the Roller Racer. For the developed prototype of the robot, the most optimal control parameters which ensure the maximum average velocity have been found. Combining simple movements along a straight line and a circle trajectories, more complex trajectories can be designed. The results of experiments of the prototype coincide with the results of simulations. In the future, we plan to investigate more detail the curvature of the trajectory from the shift φ_0, the amplitude α, the period T and the ratios of moments of inertia J_{20}/J_{10}.

Acknowledgment. The work of A. A. Kilin (Sect. 2) is carried out in the Ural Mathematical Center. The work of Yefremov K. S. and Karavaev Y. L. (Sect. 3) was carried out within the framework of the state assignment of the Ministry of Education and Science of Russia (FZZN-2020-0011). The experimental investigations were carried out using the equipment of the Common Use Center of the Udmurt State University.

References

1. Martynenko, Y.G.: Motion control of mobile wheeled robots. J. Math. Sci. (N. Y.) **147**(2), 6569–6606 (2007)
2. Bloch, A.: Nonholonomic Mechanics and Control. Springer, Heidelberg, 501p. (2003). https://doi.org/10.1007/b97376
3. Rocard, Y.: L'instabilité en mécanique: Automobiles, avions, ponts suspendus. Masson, Paris (1954)
4. Bizyaev, I.A.: The inertial motion of a roller racer. Regul. Chaotic Dyn. **22**(3), 239–247 (2017)
5. Bizyaev, I.A., Borisov, A.V., Mamaev, I.S.: Exotic dynamics of nonholonomic roller racer with periodic control. Regul. Chaotic Dyn. **23**(7–8), 983–994 (2018)
6. Borisov, A.V., Ivanova, T.B., Karavaev, Y.L., Mamaev, I.S.: Theoretical and experimental investigations of the rolling of a ball on a rotating plane (turntable). Eur. J. Phys. **39**(6), 065001 (2018)
7. Borisov, A.V., Kilin, A.A., Karavaev, Y.L.: Retrograde motion of a rolling disk. Physics-Uspekhi **60**(9), 931–934 (2017)
8. Karavaev, Y.L., Kilin, A.A., Klekovkin, A.V.: The dynamical model of the rolling friction of spherical bodies on a plane without slipping. Russ. J. Nonlinear Dyn. **13**(4), 599–609 (2017)
9. Krishnaprasad, P.S., Tsakiris, D.P.: Oscillations, SE (2)-snakes and motion control: a study of the roller racer. Dyn. Syst.: Int. J. **16**(4), 347–397 (2001)
10. Fedonyuk, V., Tallapragada, P.: Locomotion of a compliant mechanism with nonholonomic constraints. ASME. J. Mech. Robot. **12**, 1–13 (2020). https://doi.org/10.1115/1.4046510
11. Bullo, F., Lewis, A.D.: Kinematic controllability and motion planning for the snakeboard. IEEE Trans. Autom. Control **19**, 494–498 (2003)

12. Shammas, E., de Oliveira, M.: Motion planning for the snakeboard. Int. J. Robot. Res. **31**(7), 872–885 (2012). https://doi.org/10.1177/0278364912441954
13. Bizyaev, I.A., Borisov, A.V., Mamaev, I.S.: Dynamics of the Chaplygin Sleigh on a cylinder. Regul. Chaotic Dyn. **21**(1), 136–146 (2016)
14. Ardentov, A.A., Karavaev, Y.L., Yefremov, K.S.: Euler elasticas for optimal control of the motion of mobile wheeled robots: the problem of experimental realization. Regul. Chaotic Dyn. **24**(3), 312–328 (2019). https://doi.org/10.1134/S1560354719030055
15. Yefremov, K.S., Ivanova, T.B., Kilin, A.A., Karavaev, Y.L.: Theoretical and experimental investigations of the controlled motion of the Roller Racer. In: 2020 International Conference Nonlinearity, Information and Robotics (NIR), pp. 1–5. IEEE (December 2020)